

# Metabolic response to exogenous ethanol in yeast: An in vivo NMR and mathematical modelling approach

Silvia Martini <sup>a,c</sup>, Maso Ricci <sup>a</sup>, Fiora Bartolini <sup>a</sup>, Claudia Bonechi <sup>a</sup>, Daniela Braconi <sup>b</sup>, Lia Millucci <sup>b</sup>, Annalisa Santucci <sup>b</sup>, Claudio Rossi <sup>a,\*</sup>

<sup>a</sup> Dipartimento di Scienze e Tecnologie Chimiche e dei Biosistemi, Università di Siena Via Aldo Moro, 2-53100 Siena, Italy

<sup>b</sup> Dipartimento di Biologia Molecolare, Università di Siena Via Fiorentina, 1-53100 Siena, Italy

<sup>c</sup> Polo Universitario di Colle di Val D'Elsa Viale Matteotti, 12-53034-Colle di Val D'Elsa, Siena, Italy

Received 10 June 2005; received in revised form 10 October 2005; accepted 14 October 2005

Available online 28 November 2005

## Abstract

The understanding of the metabolic behaviour of complex systems such as eukaryotic cells needs the development of new approaches that are able to deal with the complexity due to a large number of interactions within the system. In this paper, we applied an approach based on the combined use of in vivo NMR experiments and mathematical modelling in order to analyze the metabolic response to ethanol stress in a wild-strain of *Saccharomyces cerevisiae*. Considering the cellular metabolic processes resulting from activation, inhibition, and feed-back activities, we developed a model able to describe the modulation of the whole system induced by an external stress due to increasing concentrations of exogenous ethanol. This approach was able to interpret the experimental results in terms of metabolic response to exogenous ethanol in the yeast. The robustness and flexibility of the model enables it to work correctly at different initial exogenous ethanol concentrations.

© 2005 Elsevier B.V. All rights reserved.

**Keywords:** *Saccharomyces cerevisiae*; Metabolism; Mathematical modelling; Inhibition; In vivo NMR

## 1. Introduction

Due to the exposure to specific environmental stresses, microorganisms have to provide adaptive responses [1–3]. *Saccharomyces cerevisiae* represents an ideal eukaryotic model system to investigate the effects of stress conditions on metabolic processes. Among a great variety of physical, chemical, and biological injuries which yeast cells can experience, ethanol represents the main source of stress during fermentation [4–6]. The toxic effects of ethanol on *S. cerevisiae* cells are known, and involve the modification of membrane lipid composition, the synthesis of stress proteins, modulation of ion exchange processes, as well as a reduction of metabolic activity which causes the inhibition of glucose uptake, decreasing of growth rate, and product formation [7,8].

Literature provides a large number of studies which explain the processes taking place at the molecular level during *S.*

*cerevisiae* adaptive efforts in response to external stimuli [4,9–19] as well as theoretical models able to describe and understand the complex network of interactions among the different components within the system [20–22].

In this study we propose an approach to investigate the effects of the presence of external stresses on *S. cerevisiae* glucose degradation. In particular, the combined use of in vivo <sup>13</sup>C NMR spectroscopy and mathematical modelling, allowed the evaluation of the changes in the metabolic yield of a wild-type strain of *S. cerevisiae* fermentation process due to the presence of exogenous ethanol. Because of its “non invasive” nature, NMR spectroscopy can be useful in kinetic studies in which several samplings are required during metabolic activity. In fact, the use of selective enriched substrates allow the mapping of the fate of the metabolite during the fermentation process [23–25].

Experimental NMR data, related to glucose consumption and ethanol production, were used in the present work to build a mathematical model able to simulate the yeast metabolism through fluxes of energy and matter within the system [20,21,26,27].

\* Corresponding author. Tel.: +39 0577234355; fax: +39 0577234177.

E-mail address: [rossi@unisi.it](mailto:rossi@unisi.it) (C. Rossi).

We also adopted the diagramming methodology introduced by H.T. Odum in order to highlight metabolic pathways involved in the fermentative process and including the feedback effects due to the presence of exogenous and endogenous ethanol. [28]. In particular, this approach was conceived to develop a flexible compartmental model, providing several new points of view on the complex behaviour of cell metabolism: i) the metabolisation process was described using concise symbols for energy and fluxes within the system and all main events related to glucose metabolism that occur in the cell culture; ii) a set of non-linear differential equations was developed in order to describe the time evolution of the system; iii) specific kinetic constants, associated with the non-linear differential equations and having a specific biological meaning, were calculated by a fitting procedure [29].

The model includes different compartments: the carbon source (e.g. glucose), the main fermentation product (e.g. ethanol), and the number of active yeast cells (i.e. the number of cells capable to degrade glucose), which interact exchanging energy and matter during the biochemical phenomena involved in the degradation processes. The calculation of the kinetic constant associated to the degradation of glucose,  $k_D$ , and the one related to the ethanol production,  $k_P$ , allowed the estimation of the metabolic yield response of the yeast to the inhibition effects due to an exogenous stress within the system. In fact, the presence of ethanol affected the growth rate of yeast cells, with a decreased amount of produced ethanol at the end of fermentation.

We found that increasing concentrations of exogenous ethanol lowered the metabolic yield, calculated from the ratio between the concentration (expressed in g/l) of the produced ethanol and the consumed glucose, from 90% in the absence of ethanol to about 27% in the presence of 75 g/l of exogenous ethanol.

The fitting of the calculated metabolic yield in relation to the concentration of exogenous ethanol allowed the simulation of the effects of any exogenous ethanol concentration between 0 and 75 g/l, in terms of cellular activity, glucose and ethanol concentrations as well as metabolic yield.

## 2. Materials and methods

### 2.1. Yeast strain and culture conditions

*S. cerevisiae* K310 strain was isolated from spontaneous wine fermentation [4,30] K310 was grown in YPD (Yeast Peptone Dextrose) at 30 °C with rotary shaking up to saturation ( $1 \times 10^8$  cells/ml). An aliquot of the saturated culture was inoculated in YPD, adjusted to final pH 4.5 by adding 0.2 M citrate–phosphate buffer and containing 100 g/l unlabelled glucose. The cell suspension was incubated at 25 °C without shaking (semiaerobiosis) for 10 h.

Samples were then collected and the growth steps were monitored by measuring the absorbance of the culture at 660 nm.

### 2.2. NMR measurements and mathematical modelling

K310 cell suspension at  $1 \times 10^6$  cells/ml, indicating an early log phase of growth, was centrifuged for 5 min at room temperature and  $3000 \times g$  in a Beckman centrifuge model J2-21 equipped with a JA10 rotor. The supernatant was discarded and the pellet was resuspended in the same medium containing 100 g/l of 1- $^{13}\text{C}$  glucose. 20% (v/v) of  $\text{D}_2\text{O}$  was added. Four sets of experiments were conducted. In each set the cells were placed in the same batch conditions except for the exogenous ethanol dilution rate which was 0, 20, 50 and 75 g/l, respectively.  $^{13}\text{C}$  spectra were collected with a Bruker Avance DRX 600 spectrometer operating at 600 and 150 MHz for proton and carbon nuclei, respectively. Carbon spectra were recorded under continuous broad-band decoupling conditions at time intervals of about 3 min. During the experiment the NMR probe was thermostated at 30 °C. The substrate and the end-product concentrations were calculated from the area of NMR peaks through an appropriate calibration. The total ethanol concentration was estimated by an enzymatic assay by Sigma-Aldrich (kit cod. 332-C). The fitting procedure of experimental data was performed using the program MLAB [31]. A parallel growth was carried out during the yeast growth under the NMR monitoring. Samples were collected at time 0 and after 12, 16, 19, 22, 27, 36, 44, 50, and 62 h. At each sampling the pH of the cell suspension was checked and growth was monitored by measuring the absorbance of the culture at 660 nm (results not shown). The pH (4.5) never changed during cell growth, as also already reported [4].

All high purity reagents were from Sigma-Aldrich (Milano, Italy), Merck Eurolab (Milano, Italy), Carlo Erba (Rodano, MI, Italy), Serva (Heidelberg, D). All the water used was Milli-Q quality (Millipore, Bedford, USA). 1- $^{13}\text{C}$  glucose was from Cambridge Isotope Laboratories (Andover, MA, USA).

## 3. Results and discussion

Fig. 1 reports the carbon-13 spectra displayed at time intervals of about 20 min showing the metabolisation process of 100 g/l of glucose by *S. cerevisiae*, which transfers the [1- $^{13}\text{C}$ ] glucose labelled carbon nuclei to the methyl group of ethanol.

Due to the high initial concentration of glucose, we assumed that the main metabolic pathway for the degradation of this substrate was the fermentation. In fact, when yeast grows in the presence of high glucose concentrations, the negative impact exerted by the sugar on the other metabolic pathways makes the fermentation the sole degradation pathway. Thus, we considered glucose as the unique carbon source and ethanol as the main end product of the fermentative process [32,33].

Fig. 2 shows the experimental data of glucose and ethanol concentrations in relation to time for four different experiments in which the fermentation process of 100 g/l of glucose was carried out in the presence of 0, 20, 50, and 75 g/l of exogenous ethanol, respectively. Data show that the kinetics of glucose degradation and ethanol production were strongly affected by the presence of the external perturbation. In fact, in the absence of exogenous ethanol, the fermentation process ended after

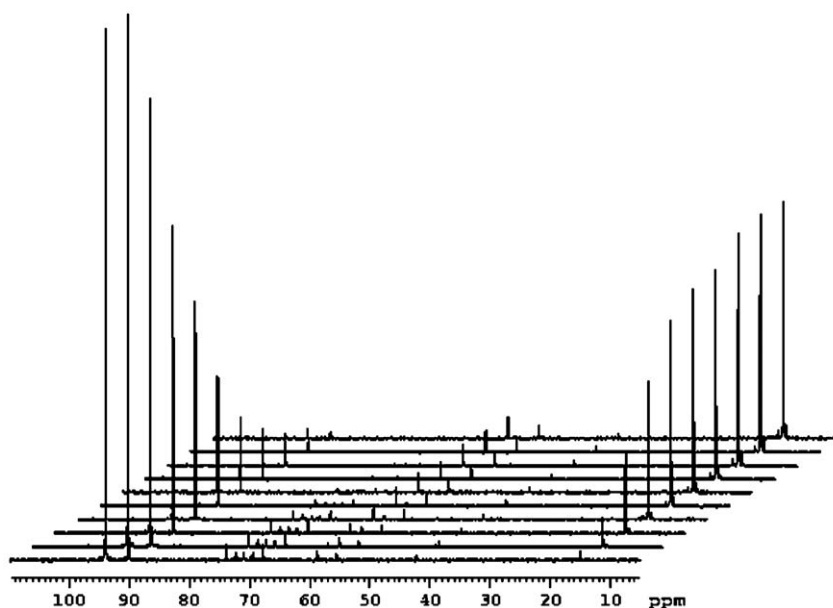


Fig. 1.  $^{13}\text{C}$ -NMR spectra obtained at 20 min intervals during glucose fermentation by *S. cerevisiae*.

about 40 h to yield 45 g/l of endogenous ethanol, while in the presence of 20, 50, and 75 g/l, glucose consumption ended after 48, 62, and 80 h, respectively, producing 41, 28, and 14 g/l of endogenous ethanol.

These results clearly show the main effects emerging upon addition of ethanol: a lowering in the fermentation rate, a decrease in the final concentration of the end-product, and consequently a reduced efficiency of the fermentation process.

### 3.1. The modelling approach

The experimental evidences obtained from *in vivo* NMR data were the basis for developing the *Energy System Diagram* of the glucose conversion by *S. cerevisiae* reported in Fig. 3.

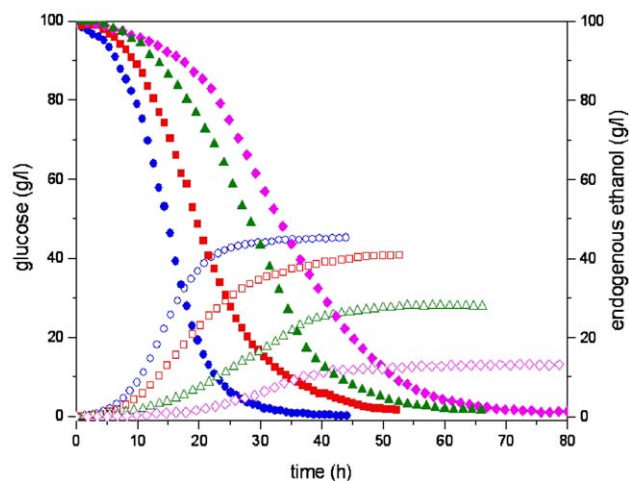


Fig. 2. (a) Data comparison of glucose (●) and ethanol (▼) concentration collected in the presence of increasing exogenous ethanol concentrations. Experiments were performed with 0 g/l of exogenous ethanol (blue data), 20 g/l of exogenous ethanol (red), 50 g/l of exogenous ethanol (green) and 75 g/l of exogenous ethanol (pink). (For interpretation of the references to colour in this figure legend, the reader is referred to the web version of this article.)

The model is composed by a few elements: glucose concentration, total ethanol concentration (which involves two distinct compartments referring to exogenous and endogenous ethanol concentrations), and an index related to the number of active cells modulated by the inhibition processes due to the presence of ethanol. An important feature of the model is the

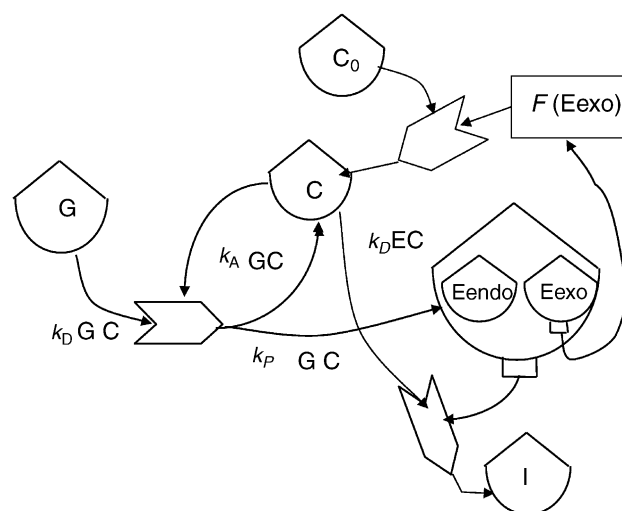


Fig. 3. Energy System Diagram of the model of fermentative process in the presence of exogenous ethanol. The diagram is composed by a few compartments representing glucose concentration ( $G$ ), total ethanol concentration which involves two distinct compartments referring to exogenous and endogenous ethanol concentrations ( $E_{\text{exo}}$  and  $E_{\text{endo}}$ , respectively), cellular activity ( $C$ ) and inhibited cells ( $I$ ) (not included in the set of differential equations). The fluxes and interactions among the compartments are symbolized by arrows. The dynamics of glucose metabolism was assumed to be the result of an autocatalytic process which depends on the concentration of the available carbon source and the cellular activity. The presence of the sugar promotes an energy flow to the active cells which allows the cell culture to grow. The interaction between the total ethanol and the number of actual active cells takes into account the inhibition effects which produced the amount of inhibited cells during the fermentation.

ability to consider the extent of the damage caused by the addition of exogenous ethanol on the cell culture at time zero. In fact, the effective number of cells able to carry out the fermentation depends on the amount of exogenous ethanol added to the system at the beginning of the experiment. The dynamics of glucose metabolism was assumed to be the result of an autocatalytic process which depends on the concentration of the available carbon source and the cellular activity. The presence of the sugar promotes an energy flow to the active cells which allows the cell culture to grow.

The interaction between the total ethanol and the number of actual active cells takes into account the inhibition effects which produced the amount of inhibited cells during the fermentation.

The entire system is represented by a set of non-linear differential equations as follows:

$$\frac{dG}{dt} = -k_D[G][C] \quad (1)$$

$$\frac{dE_{\text{endo}}}{dt} = k_P[G][C] \quad (2)$$

$$\frac{dC}{dt} = k_A[G][C] - k_I\{[E_{\text{exo}}] + [E_{\text{endo}}]\}[C] \quad (3)$$

$$[C]_{t=0} = [C_0] \frac{1}{1 + h[E_{\text{exo}}]} \quad (4)$$

where  $[G]$ ,  $[E_{\text{endo}}]$  and  $[E_{\text{exo}}]$  are the concentrations of glucose, endogenous and exogenous ethanol, respectively.  $[C]$  is the cellular activity during fermentation,  $[C]_{t=0}$  is the initial cellular activity, and  $[C_0]$  is the cellular activity in the absence of exogenous ethanol. In this work we consider the “cellular activity” as an adimensional index related to the concentration of cells capable to carry out the fermentation process. At time zero, in the presence of exogenous ethanol, the initial concentration of cells is the same as in the absence of ethanol, but the concentration of “active cells” (i.e. the cellular activity) decreases according to Eq. (4).

Both the rates of glucose degradation and ethanol production are related to glucose concentration and cellular activity (Eqs. (1) and (2)). Ethanol acts as an inhibition factor modulating the cellular activity  $[C]$  (Eq. (4)).

$k_i$  (with  $i=D, A, P, I$ ) represents the kinetic constants associated with the degradation of glucose ( $k_D$ ), production of ethanol ( $k_P$ ), cellular activation ( $k_A$ ) promoted by the substrate, and cellular inhibition ( $k_I$ ) due to the total ethanol within the system.

The constant  $h$  (Eq. (4)) is referred to a function which controls the initial concentration of active cells ( $[C]_{t=0}$ ) in the presence of exogenous ethanol, which reduces the cellular activity at the beginning of the fermentation.

In the absence of exogenous stress, the initial cellular activity is assumed to be 1; as the concentration of the stress source increases, the value of  $[C]_{t=0}$  decreases. Cellular activity  $[C]$  includes the inhibitory effects exerted by exogenous ethanol at the beginning of the process as well as the negative feedback due to the increasing amount of ethanol during fermentation.

The validity of the model was checked against experimental data. The constants in each equation were optimised by a non linear least-square estimation technique as implemented in MLAB computer program using the Marquardt–Levenberg method aiming the best fit between measured and predicted values of glucose and produced ethanol concentrations [32].

The four sets of experimental data were used simultaneously to calculate the constants  $k_D$ ,  $k_A$ ,  $k_I$ ,  $h$ , and  $k_P$ , this last one calculated for each set of data. Fig. 4 (panels A–D) reports the experimental and calculated data of glucose consumption and ethanol production for different concentrations of exogenous ethanol. The results showed an excellent agreement between simulated and experimental data for both glucose and ethanol ( $R^2=0.995$ ).

Some interesting aspects of the phenomena under study can be investigated by analysing the values of the constants calculated from the model (Table 1). In particular,  $k_D$ , the constant related to the degradation of glucose, assumes the same value for the three sets of data suggesting that the lowering of the fermentation rate observed in the presence of exogenous ethanol was only due to a decreasing of the cellular activity at the beginning of the fermentation. In fact, experimental data showed that the yeast cells completely degraded the substrate even in the presence of the stress source, implying that the concentration of active cells represents the sole variable capable to affect the rate of glucose degradation. The kinetic constant associated to ethanol production,  $k_P$ , represents an index related to the ethanol production efficiency in the presence of exogenous ethanol. As noted above, the yielded ethanol at the end of the fermentation was different, depending on exogenous ethanol concentration. According to the experimental results, the calculated  $k_P$  values decreased with increasing exogenous ethanol concentration. This suggests that the stress induced by the presence of ethanol reduces the fermentative ability causing the lowering of the production rate and the final concentration of ethanol. Fig. 5 shows the simulated behaviour of cellular activity calculated for each experiment in relation to time, as the result of two contributions: at the beginning of fermentation the high glucose concentration induces the increase of cellular activity with a rate equal to the activation parameter  $k_A$ , while an opposite effect is induced by the produced ethanol which inhibits the fermentation process causing a decrease in the cellular activity with a rate equal to the inhibition parameter  $k_I$ . As expected,  $k_A$  assumes higher values than  $k_I$ , so that the ability of glucose in promoting the fermentation process is greater than the feed-back inhibition due to the presence of ethanol, causing this curve to be non symmetrical in respect to time. The maximum value reached by each curve decreased with increasing ethanol concentration, in agreement with the lower fermentation rate observed in the experimental data.

### 3.2. Further development of the model

Let us consider the bioconversion of glucose into ethanol occurring during the fermentation process:



The theoretical metabolic yield of the process can be calculated from the ratio between the weight of two moles of ethanol



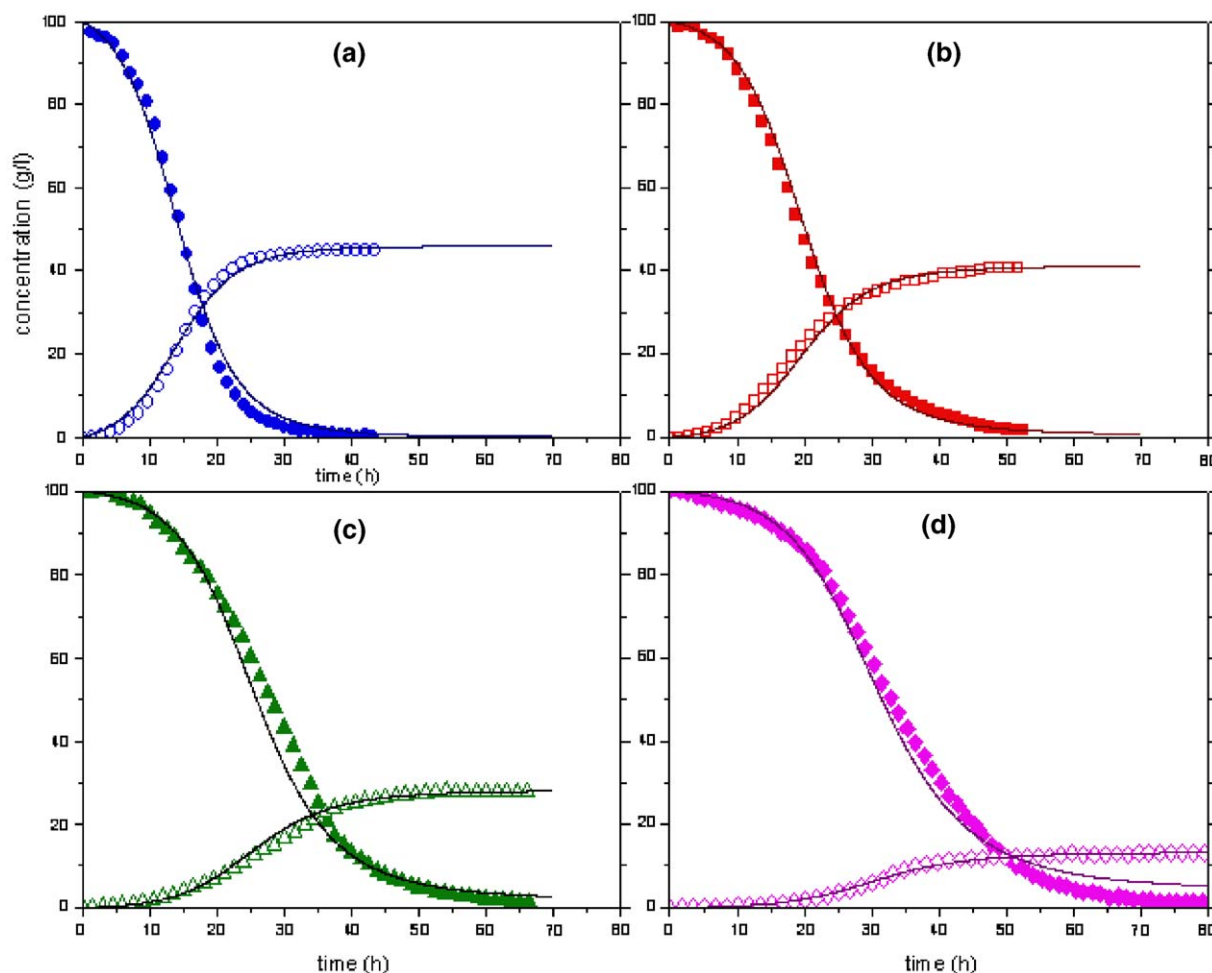


Fig. 4. Experimental time course of ethanol (▼) and glucose (●) compared with model simulation (continuous line). (a) In the absence of exogenous ethanol (blue data); (b) in the presence of 20 g/l of ethanol (red); (c) in the presence of 20 g/l of ethanol (green); (d) in the presence of 75 g/l of ethanol (pink). (For interpretation of the references to colour in this figure legend, the reader is referred to the web version of this article.)

(i.e. 92 g) and one mole of glucose (i.e. 180 g), which gives a value of 0.51 that represents the maximum achievable yield.

The experimental metabolic yield (EMY) for the four different systems can be obtained from the ratio between the produced ethanol and the glucose concentrations. Fig. 6 reports the plot of endogenous ethanol concentration vs. metabolized glucose concentration in the absence of exogenous ethanol (a) and in the presence of 20 (b), 50 (c), and 75 g/l (d) of ethanol. The figure also reports the slopes of the straight lines which represent the values of EMY for the fermentation process

carried out in different stress conditions. Results show that the yield of the fermentation process decreased with increasing exogenous ethanol concentration, and reaches the minimum

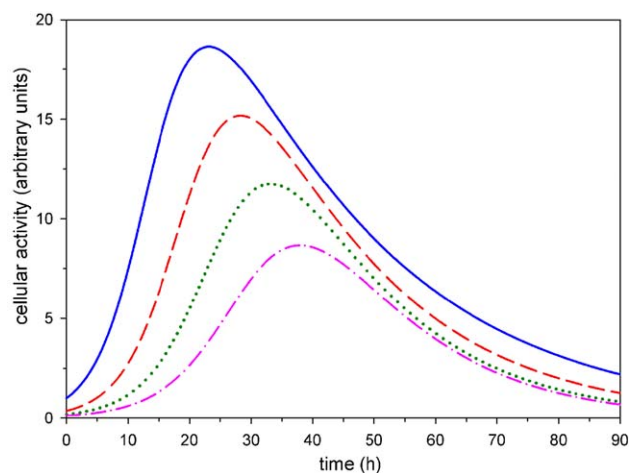


Fig. 5. Cellular activity curves simulated by the model: in the absence of exogenous ethanol (blue), at 20, 50 and 75 g/l of exogenous ethanol (red, green and pink lines, respectively). (For interpretation of the references to colour in this figure legend, the reader is referred to the web version of this article.)

Table 1  
Estimated values and coefficient of variation (CV) of the kinetics parameters

Parameters	Units	Value	CV (%)
$k_D$	$s^{-1}$	$2.58 \cdot 10^{-06}$	0.93
$k_{P0}$	$s^{-1}$	$1.18 \cdot 10^{-06}$	0.94
$k_{P20}$	$s^{-1}$	$1.08 \cdot 10^{-06}$	0.97
$k_{P50}$	$s^{-1}$	$7.49 \cdot 10^{-07}$	0.98
$k_{P75}$	$s^{-1}$	$3.57 \cdot 10^{-07}$	1.08
$k_A$	$l \cdot g^{-1} \cdot s^{-1}$	$6.21 \cdot 10^{-07}$	0.36
$k_1$	$l \cdot g^{-1} \cdot s^{-1}$	$2.19 \cdot 10^{-07}$	0.74
$h$	$l \cdot g^{-1}$	$9.80 \cdot 10^{-02}$	0.89

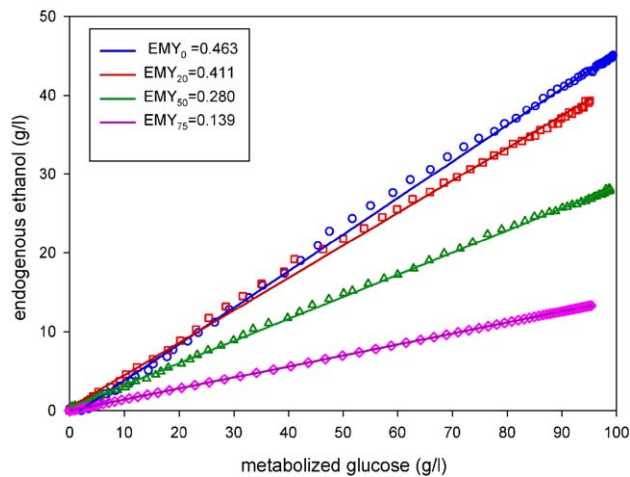


Fig. 6. Plot of endogenous ethanol vs. consumed glucose concentration for the fermentation process of 100 g/l of glucose: (blue) in the absence of exogenous ethanol, (red) in the presence of 20 g/l of ethanol, (green) in the presence of 50 g/l of ethanol and (pink) in the presence of 75 g/l of ethanol. The slope of each line calculated by linear regression of experimental data is also reported as EMY0, EMY20, EMY50 and EMY75. (For interpretation of the references to colour in this figure legend, the reader is referred to the web version of this article.)

efficiency (about 27% of the maximum achievable yield) in the presence of 75 g/l of ethanol.

The analysis of the values of the kinetic parameters obtained by mathematical modelling allows the interpretation of the response of the yeast to the stress conditions applied to the systems as well as the estimation of the metabolic yield of the four processes. For this purpose, we can use Eqs. (1) and (2) in order to calculate the yield of the fermentation from the ratio between the amount of ethanol produced and the glucose consumed during the degradation process:

$$dG = -k_D[G][C]dt$$

$$dE = k_p[G][C]dt$$

then

$$\frac{dE}{dG} = -\frac{k_p}{k_D} \tag{6}$$

The ethanol produced and the glucose consumed by fermentation can be explicated in terms of finite variations:

$$\frac{\Delta E}{\Delta G} = \left| -\frac{k_p}{k_D} \right| = Y_M \tag{6b}$$

Table 2  
Experimental metabolic yield (EMY) and metabolic yield calculated from the model ( $Y_M$ )

Exogenous ethanol (g/l)	EMY	$Y_M$
0	0.463	0.462
20	0.411	0.422
50	0.280	0.291
75	0.139	0.138

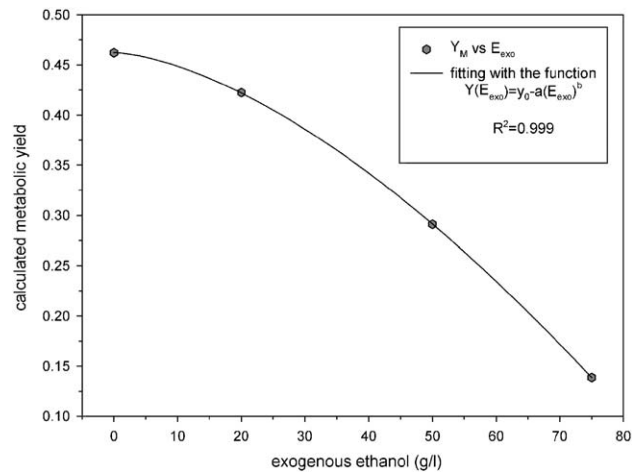


Fig. 7. Calculated metabolic yield ( $Y_M$ ) in relation to exogenous ethanol concentration and data fitting.

If we substitute the expression of  $k_P$  in Eq. (2) we obtain:

$$\frac{dE}{dt} = Y_M k_D [G][C] \tag{7}$$

Relation (6) shows that it is possible to derive the metabolic yield of each process simply by calculating the ratio between the kinetic constants associated to ethanol formation and the glucose consumption. These results, obtained from the mathematical model ( $Y_M$ ), were compared to the values obtained from experimental data (EMY) in Table 2. The comparison between the two sets of results suggests that the developed model is able to interpret coherently the behaviour of the yeast cells in the presence of different concentrations of exogenous ethanol and to describe the stress effects in terms of decreased metabolic activity in perfect agreement with the experimental results.

3.3. Predictive ability of the model

Fig. 7 reports the values of the calculated metabolic yield ( $Y_M$ ) vs. exogenous ethanol concentration. The relation

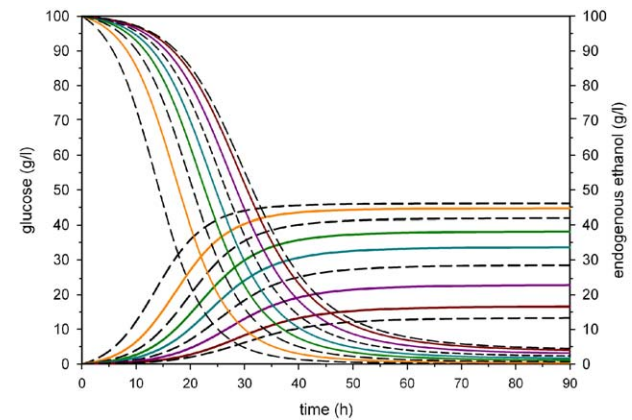


Fig. 8. Simulation of glucose degradation and ethanol formation during the fermentative process in the presence of 0, 10, 20, 30, 40, 50, 60, 70, 75 g/l of exogenous ethanol. The coloured line plots are calculated by fitting the experimental data, the black ones are simulated by the model.

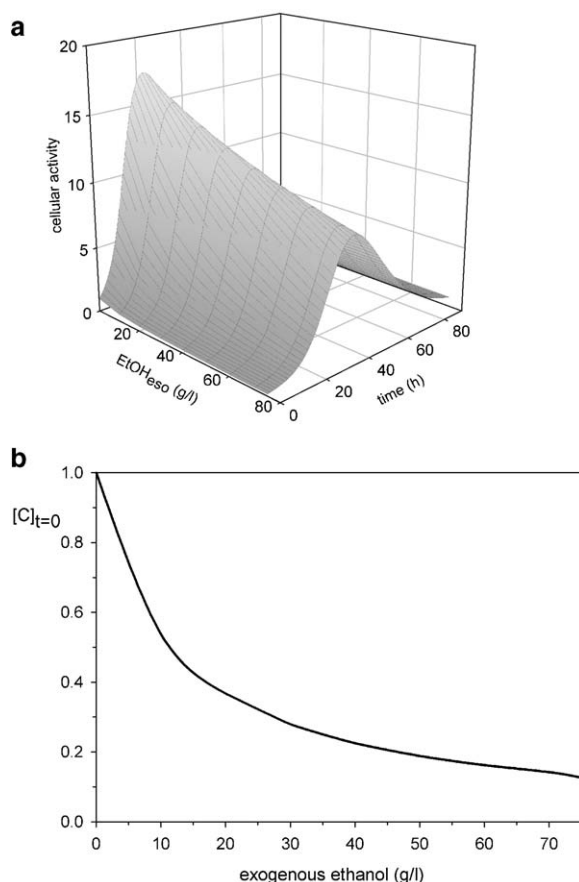


Fig. 9. (a) 3D plot of cellular activity vs. time and exogenous ethanol concentration and (b) simulation of the cellular activity vs. time.

between  $Y_M$  and the exogenous ethanol concentration ( $E_{\text{exo}}$ ) can be described by the following function:

$$g(E_{\text{exo}}) = y_0 - a(E_{\text{exo}})^b \quad (8)$$

The values of the parameters of this equation, calculated by the fitting procedure, are:

$$y_0 = 0.461$$

$$a = 6.28 \times 10^{-4} (1/\text{g})^b$$

$$b = 1.436$$

The result of the fitting procedure is also reported in Fig. 7. Substituting function (8) in Eq. (7) we obtain:

$$\frac{dE}{dt} = [y_0 - a(E_{\text{exo}})^b] k_D [G][C] \quad (9)$$

Once the model is updated with this differential equation, it succeeds in simulating the glucose and ethanol dynamics and the cellular activity at any exogenous ethanol concentration. Fig. 8 reports the simulations for glucose degradation and ethanol formation in the presence of 0, 10, 20, 30, 40, 50, 60, 70 and 75 g/l of exogenous ethanol. The coloured line plots are

the ones calculated by fitting of the experimental data (0, 20, 50 and 75 g/l), while the black line plots are estimated using increasing ethanol concentration values in Eq. (9).

The model, including Eq. (9), also allows the simulation of the cellular activity in relation to time and exogenous ethanol concentration, as shown in the 3D-graph of Fig. 9a. Fig. 9b shows the simulation of the initial cellular activity value ( $[C]_{t=0}$ ) calculated by the mathematical model in relation to exogenous ethanol concentration. As predicted before (Eq. (4)), the value of  $[C]_{t=0}$  equals 1 in absence of external stress and decreases as the exogenous ethanol concentration increases, thus inducing an initial stress on cell culture.

#### 4. Conclusions

The combined use of mathematical modelling and in vivo  $^{13}\text{C}$  NMR spectroscopy allowed the analysis of the response to ethanol stress in a wild-type strain of *S. cerevisiae*, in terms of a reduced metabolic activity. The model developed succeeded in describing and interpreting the effects of increasing concentrations of exogenous ethanol. The ratio between the kinetic constants associated to the ethanol production ( $k_P$ ) and glucose consumption ( $k_D$ ) gave the estimation of the metabolic yield of the processes in perfect agreement with experimental results. This parameter allowed the simulation of the system response to any exogenous ethanol concentration between 0 and 75 g/l.

#### Acknowledgments

This work was supported by MIUR Fondo per gli Investimenti della Ricerca di Base (FIRB), n. RBAU01JE9A, Italian Inter-University Consortium CSGI and Fondazione Monte dei Paschi di Siena Grants 2004 and 2005.

#### References

- [1] R.M. Birch, G.M. Walker, Influence of magnesium ions on heat shock and ethanol stress responses of *Saccharomyces cerevisiae*, *Enzyme Microb. Technol.* 26 (2000) 678–687.
- [2] S. Hohmann, W.H. Mager, in: S. Hohmann, W.H. Mager (Eds.), *Yeast Stress Responses*, Springer, New York, 1997, pp. 1–5.
- [3] I.W. Dawes, in: J.R. Dickinson, M. Schweizer (Eds.), *The Metabolism and Molecular Physiology of Saccharomyces cerevisiae*, Taylor and Francis, London, 1999, pp. 277–326.
- [4] L. Trabalzini, A. Paffetti, A. Scaloni, F. Talamo, E. Ferro, G. Coratza, L. Bovolini, P. Lusini, P. Martelli, A. Santucci, Proteomic response to physiological fermentation stresses in a wild-type wine strain of *Saccharomyces cerevisiae*, *Biochem. J.* 370 (2003) 35–46.
- [5] M. Ricci, S. Martini, C. Bonechi, L. Trabalzini, A. Santucci, C. Rossi, Inhibition effects of ethanol on the kinetics of glucose metabolism by *S. cerevisiae*: NMR and modelling study, *Chem. Phys. Lett.* 387 (2004) 377–382.
- [6] S. Martini, M. Ricci, C. Bonechi, L. Trabalzini, A. Santucci, C. Rossi, In vivo  $^{13}\text{C}$ -NMR and modelling study of metabolic yield response to ethanol stress in a wild-type strain of *Saccharomyces cerevisiae*, *FEBS Lett.* 56 (2004) 63–68.
- [7] T. D'Amore, G.G. Stewart, Ethanol tolerance of yeast, *Enzyme Microb. Technol.* 9 (1987) 322–330.
- [8] H. Alexandre, V. Ansanay-Galeote, S. Dequin, B. Blondin, Global gene expression during short-term ethanol stress in *Saccharomyces cerevisiae*, *FEBS Lett.* 498 (2001) 98–103.

- [9] F. Estruch, Stress-controlled transcription factors, stress-induced genes and stress tolerance in budding yeast, *FEMS Microbiol. Rev.* 24 (2000) 469–486.
- [10] V. Costa, P. Moradas-Ferreira, Oxidative stress and signal transduction in *Saccharomyces cerevisiae*: insights into ageing, apoptosis and diseases, *Mol. Aspects. Med.* 22 (4–5) (2001) 217–246.
- [11] A.R. Barber, F. Vriesekoop, N.B. Pamment, Effects of acetaldehyde on *Saccharomyces cerevisiae* exposed to a range of chemical and environmental stresses, *Enzyme Microbiol. Technol.* 30 (2002) 240–250.
- [12] P.W. Piper, The heat shock and ethanol stress responses of yeast exhibit extensive similarity and functional overlap, *FEMS Microbiol. Lett.* 134 (1995) 121–127.
- [13] K.W. Wirtz, A generic model for changes in microbial kinetic coefficients, *J. Biotechnol.* 97 (2002) 147–162.
- [14] W. Wiechert, Modeling and simulation: tools for metabolic engineering, *J. Biotechnol.* 94 (2002) 37–63.
- [15] P.P.F. Hanegraaf, A.H. Stouthamer, Kooijman, S.A.L.M., a mathematical model for yeast respiration-fermentative physiology, *Yeast* 16 (2000) 423–437.
- [16] R. Heinrich, S. Schuster, The modelling of metabolic system. Structure, control and optimality, *BioSystems* 47 (1998) 61–77.
- [17] B. Teusink, J. Passarge, C.A. Reijenga, E. Esgalhado, C.C. van der Weijden, M. Schepper, M.C. Walsh, B.M. Bakker, K. van Dam, H.V. Westerhoff, J.L. Snoep, Can yeast glycolysis be understood in terms of in vitro kinetics of the constituent enzymes? Testing biochemistry, *Eur. J. Biochem.* 267 (2000) 5313–5329.
- [18] F. Alvarez-Vasquez, K.J. Sims, L.A. Cowart, Y. Okamoto, E.O. Voit, Y.A. Hannun, Simulation and validation of modelled sphingolipid metabolism in *Saccharomyces cerevisiae*, *Nature* 433 (2005) 425–430.
- [19] F. Alvarez-Vasquez, K.J. Sims, Y.A. Hannun, E.O. Voit, Integration of kinetic information on yeast sphingolipid metabolism in dynamical pathway models, *J. Theor. Biol.* 226 (2004) 265–291.
- [20] S. Bastianoni, A. Donati, A. Gastaldelli, N. Marchettini, D. Renzoni, C. Rossi, Modeling interpretation of microbe metabolism detected by nuclear magnetic resonance, *Biochem. Biophys. Res. Commun.* 227 (1996) 53–58.
- [21] S. Bastianoni, A. Gastaldelli, C. Bonechi, C. Mocenni, C. Rossi, Kinetic analysis and comparison of models of xylose metabolism by *Klebsiella planticola*, *Biochem. Biophys. Res. Commun.* 227 (1996) 41–46.
- [22] E. Klipp, B. Nordlander, R. Kruger, P. Gennemark, S. Hohmann, Integrative model of the response of yeast to osmotic shock, *Nat. Biotechnol.* 23 (8) (2005).
- [23] J.A. den Hollander, T.R. Brown, K. Ugurbil, R.G. Shulman, <sup>13</sup>C nuclear magnetic resonance studies of anaerobic glycolysis in suspensions of yeast cells, *Proc. Natl. Acad. Sci. U. S. A.* 205 (1979) 6096–6100.
- [24] R.G. Shulman, T.R. Brown, K. Ugurbil, S. Ogawa, S.M. Cohen, J.A. denHollander, Cellular applications of <sup>31</sup>P and <sup>13</sup>C nuclear magnetic resonance, *Science* 205 (1979) 160–166.
- [25] R.G. Shulman, NMR spectroscopy of living cells, *Sci. Am.* 248 (1983) 86–93.
- [26] S. Bastianoni, A. Donati, A. Gastaldelli, N. Marchettini, S. Martini, C. Rossi, A modellistic view of the kinetics of metabolic processes: differences in the glucose and xylose degradation pathway, *Chem. Phys. Lett.* 310 (1999) 38–42.
- [27] C. Rossi, M. Porcelli, C. Mocenni, N. Marchettini, S. Loisel, S. Bastianoni, A modelling approach for the analysis of xylose–ethanol bioconversion, *Ecol. Model.* 113 (1998) 157–162.
- [28] H.T. Odum, in: B.C. Patten (Ed.), *System Analysis and Simulation in Ecology*, vol. 2, Academic Press, New York, 1972, pp. 139–211.
- [29] S. Bastianoni, C. Bonechi, A. Gastaldelli, S. Martini, C. Rossi, in: A. Poggi (Ed.), *Modelling Interpretation of the Kinetics of Metabolic Processes in Chemistry at the Beginning of the Third Millennium: Molecular Design, Supramolecules, Nanotechnology and Beyond*, Springer Verlag, Berlin/Heidelberg, Germany, 2000, pp. 305–328.
- [30] A. Santucci, L. Trabalzini, L. Bovalini, E. Ferro, P. Neri, P. Martelli, Differences between predicted and observed sequences in *Saccharomyces cerevisiae*, *Electrophoresis* 21 (17) (2000) 3717–3723.
- [31] B. Bunow, G. Knott, MLAB, a Mathematical Modeling Laboratory, Civilized Software Inc., Bethesda, MD, 1992.
- [32] R.H. De Deken, The Crabtree effect: a regulatory system in yeast, *J. Gen. Microbiol.* 44 (1996) 149–156.
- [33] A. Fiechter, G.F. Fuhrmann, O. Kappeli, Regulation of glucose metabolism in growing yeast cells, *Adv. Microb. Physiol.* 22 (1981) 123–183.